IJO - INTERNATIONAL JOURNAL OF MATHEMATICS

(ISSN: 2992-4421) Prakasha.P[1]*

https://ijojournals.com/ Volume 07 Issue 04 || April, 2024 ||

Mathematical Analysis of Effect of Viscous dissipation on Transient MHD convective Heat transfer through a porous medium in a vertical channel

Mathematical Analysis of Effect of Viscous dissipation on Transient MHD convective Heat transfer through a porous medium in a vertical channel

Prakasha.P[1], Prof. K. Shivashankara[2], Venuprasad K. K.[3], Dhananjaiah D. S[4].

[1]Department of Mathematics, Government First Grade College, Magadi, Ramanagar, India
E-mail id: profprakasha@gmail.com

[2]Department of Mathematics, Yuvaraja's College, University of Mysore, Mysore, India
E-mail id: drksshankara@gmail.com

[3]Department of Mathematics, Government First Grade College K.R.Pete, Mandya, India
E-mail id: kkvpmaths@gmail.com

[4]Department of Mathematics, Government First Grade College K.R.Nagar, Mysuru, India
E-mail id: dhanu2614@gmail.com

Abstract: We analysed the unsteady MHD free connective flow through a porous medium in a vertical channel with the unsteadiness in the flow is due to the travelling thermal wave imposed on the wall y = L. The coupled MHD equations governing the flow and heat transfer have been solved by using a perturbation technique with the aspect ratio as perturbation parameter. The expression for the velocity, the temperature, the shear stress and the rate of heat transfer are derived and are analysed for different variations of the governing parameters G,R,α and γ.

Key words: Convection, Porous medium, Magneticfield and Dissipation.

1. Introduction:

The energy crisis has been a topic of great importance in recent years all over the world .This has resulted in an unabated exploration for new ideas and avenues in harnessing various conventional energy sources like tidal waves, wind power and geothermal energy. It is well known that in order to harness maximal geothermal energy one should have complete and precise knowledge of quanta of perturbation needed to initiate convection currents in mineral fluids embedded in the earth's crest enables one to use mineral energy to extract the minerals .Convection fluid flows generated by travelling thermal waves have also received attention due to applications in physical problems. The linearised analysis of these flows has shown that a travelling thermal wave cal generate a mean shear flow within a layer of fluid, and the induced mean flow is proportional to the square of the amplitude of the wave. From a physical point of view, the motion induced by travelling thermal waves is quite interesting as a purely fluid-dynamical problem and can be used as a possible explanation for the observed four-day retrograde zonal motion of the upper atmosphere of Venus. All the above mentioned studies are based on the hypothesis that the effect of dissipation is neglected. This is possible in case of ordinary fluid flow like air and water under gravitational force .But this effect is excepted to be relevant for fluids with high values of the dynamic viscosity flows. In view if this, several authors notably Barletta [1,2], Bulent Yesilata [3] , Elhakein [4], Israel et al[5] and Rossidischio [6] have studied the effect of viscous dissipation on the convective flows past an infinite vertical plate and through vertical channels and ducts.

In recent years, a great deal of interest has been generated in the area of boundary layer flow and heat transfer of a fluid over a stretching sheet In view of its numerous and wide range of applications in various fields such as polymer processing industry in particular manufacturing

IJO - INTERNATIONAL JOURNAL OF MATHEMATICS
(ISSN: 2992-4421)
https://ijojournals.com/
Volume 07 Issue 04 || April, 2024 ||
Prakasha.P[1]*

process of artificial films, artificial fibers, and dilute polymer solutions. To be more specific, it may be pointed out that many metallurgical processes involve the cooling of continuous strips or filaments by drawing them through a quiescent fluid, and in the process of drawing, these strips are sometimes stretched. The heat transfer analysis over a stretching surface is of much practical interest due to its abundant applications such as heat-treated materials travelling between a feed roll and wind-up roll or materials manufactured by extrusion, glass-fiber, and paper production, cooling of metallic sheets or electronic chips, drawing of plastic films, liquid films in condensation processes. Due to the high applicability of this problem in the industrial phenomena, it has attracted attention of many researchers.

The effects of the buoyancy force on the development of the velocity and thermal boundary layer flows over a stretching sheet were first studied by Chen[7]. Elbashbeshy and Bazid[8], Sharidan et al.[9], and Tsai et al.[10] obtained a similarity solution for the flow and heat transfer of a fluid over an unsteady stretching surface. The problem of mixedconvection adjacent to a vertical continuously stretching sheet in the presence of a variable magnetic field was studied by Ishak et al.[11]. Aziz[12] obtained the numerical solution for the laminar thermal boundary over a flat plate with a convective surface boundary conditions.

The effect of viscous dissipation changes the temperature distributions by playing a role as an energy source, which affects the heat transfer rates. The merit of the effect of viscous dissipation depends on whether the plate is being cooled or heated. Chen[13] examined the effect of combined heat and mass transfer on magnetohydrodynamic (MHD) free convection from a vertical surface with the Ohmic heating and viscous dissipation. Pal and Hiremath[14] determined the heat transfer characteristics in the laminar boundary layer flow over an unsteady stretching sheet placed in a porous medium in the presence of viscous dissipation and internal absorption or generation.

Veena et al.[15] obtained the solutions of heat transfer in a visco-elastic fluid past a stretching sheet with viscous dissipation and internal heat generation.In light of the above investigations, it is found that these studies are restricted to the fluid flow and heat transfer problems. However, the fluid flow embedded with dust particles is encountered in different engineering problems concerned with nuclear reactor cooling, powder technology, rain erosion, paint spraying, etc. The important applications of dust particles in the boundary layer include soil erosion by natural winds and dust entrainment in a cloud during a nuclear explosion. It also occurs in awide range of technical processes like fluidization, flow in rocket tubes, combustion, and purification of crude oil. Palani and Ganesan[16] investigated the flow of dusty gas past a semi-infinite isothermal inclined plate.

2. Mathematical formulation :

We consider the motion of viscous, incompressible fluid through a porous medium in a vertical channel bounded by flat walls . The thermal buoyancy in the flow field is created by a travelling thermal wave imposed on the boundary wall at $y = L$ while the boundary at $y = -L$ is maintained at constant temperature T_1. The viscous and Darcy dissipations are taken into account to the transport of heat by conduction and convection in the energy equation. Also the kinematic viscosity ν,the thermal conducting k are treated as constants. We choose a rectangular Cartesian system 0 (x ,y) with x-axis in the vertical direction and y-axis normal to the walls.

The equations governing the unsteady flow and heat transfer under boundary conditions in terms of stream function ψ are

IJO - INTERNATIONAL JOURNAL OF MATHEMATICS
(ISSN: 2992-4421)
https://ijojournals.com/
Volume 07 Issue 04 || April, 2024 ||

$$[(\nabla^2\psi)_t+\psi_x(\nabla^2\psi)_y-\psi_y(\nabla^2\psi)_x]=\nu\nabla^4\psi-\beta g(T-T_0)_y-\left(\frac{\sigma\mu_e^2H_0^2}{\rho_0}\right)\frac{\partial^2\psi}{\partial y^2}-\left(\frac{\nu}{k}\right)\nabla^2\psi \quad (2.1)$$

$$\rho_e C_p\left(\frac{\partial\theta}{\partial t}+\frac{\partial\psi}{\partial y}\frac{\partial\theta}{\partial x}-\frac{\partial\psi}{\partial x}\frac{\partial\theta}{\partial y}\right)=\lambda\nabla^2\theta+Q+\mu\left(\left(\frac{\partial^2\psi}{\partial y^2}\right)^2+\left(\frac{\partial^2\psi}{\partial x^2}\right)^2\right)+ + \left(\frac{\mu}{k}+\sigma\mu_e^2H_0^2\right)\left(\left(\frac{\partial\psi}{\partial x}\right)^2+\left(\frac{\partial\psi}{\partial y}\right)^2\right) \quad (2.2)$$

The flow is maintained by a constant volume flux for which a characteristic velocity is defined as

$$Q=\frac{1}{2L}\int_{-L}^{L}u\,dy. \quad (2.3)$$

The boundary conditions for the velocity and temperature fields are

$u=0$, $v=0$, $T=T_1$ on $y=-L$

$u=0,\ v=0,\ T=T_2+\Delta T_e\,Sin(mx+nt)$ on $y=L$ (2.4)

where $u=-\psi_y$, $v=\psi_x$ (2.5)

Introducing the non-dimensional variables in (2 .10)- (2.12) as

$$x'=mx,\ y'=y/L,\ t'=t\nu m^2,\ \psi^1=\psi/\nu,\ \theta=\frac{T-T_e}{\Delta T_e} \quad (2.6)$$

(under the equilibrium state $\Delta T_e=T_e(L)-T_e(-L)=\frac{QL^2}{\lambda}$)

the governing equations (2.1) & (2.2) in the non-dimensional form (after dropping the dashes) are

$$\delta R\left(\delta(\nabla_1^2\psi)_t+\frac{\partial(\psi,\nabla_1^2\psi)}{\partial(x,y)}\right)=\nabla_1^4\psi+\left(\frac{G}{R}\right)\theta_y-D^{-1}\nabla_1^2\psi-M^2\frac{\partial^2\psi}{\partial y^2} \quad (2.7)$$

and the energy equation in the non-dimensional form is

$$\delta P\left(\delta\frac{\partial\psi}{\partial t}+\frac{\partial\psi}{\partial y}\frac{\partial\theta}{\partial x}-\frac{\partial\psi}{\partial x}\frac{\partial\theta}{\partial y}\right)=\nabla_1^2\theta+\alpha+\left(\frac{PR^2E_c}{G}\right)\left(\left(\frac{\partial^2\psi}{\partial y^2}\right)^2+\delta^2\left(\frac{\partial^2\psi}{\partial x^2}\right)^2\right)+ +\left(D^{-1}+M^2\right)\left(\delta^2\left(\frac{\partial\psi}{\partial x}\right)^2+\left(\frac{\partial\psi}{\partial y}\right)^2\right) \quad (2.8)$$

where

$R=\frac{UL}{\nu}$ (Reynolds number),

$G=\frac{\beta g\Delta T_e L^3}{\nu^2}$ (Grashof number)

$P=\frac{\mu c_p}{k_1}$ (Prandtl number),

$D^{-1}=\frac{L^2}{k}$ (Darcy parameter),

$E_c=\frac{\beta g L^3}{C_p}$ (Eckert number),

IJO - INTERNATIONAL JOURNAL OF MATHEMATICS
(ISSN: 2992-4421)
Prakasha.P[1]*
https://ijojournals.com/ Volume 07 Issue 04 || April, 2024 ||
Mathematical Analysis of Effect of Viscous dissipation on Transient MHD convective Heat transfer through a porous medium in a vertical channel

$\delta = m\,L$ (Aspect ratio)

$\gamma = \dfrac{n}{\nu m^2}$ (non-dimensional thermal wave velocity),

$M^2 = \left(\dfrac{\sigma\mu_e^2 H_o^2 L^2}{\nu^2}\right)$ (*Hartmann Number*)

$\nabla_1^2 = \delta^2 \dfrac{\partial^2}{\partial x^2} + \dfrac{\partial^2}{\partial y^2}$

The corresponding boundary conditions are

$$\psi(+1) - \psi(-1) = 1$$

$$\frac{\partial\psi}{\partial x} = 0, \quad \frac{\partial\psi}{\partial y} = 0 \quad at\ y = \pm 1 \tag{2.9}$$

$$\theta(x, y) = 1 \qquad \text{on} \quad y = -1$$

$$\theta(x, y) = Sin(x + \gamma t) \qquad \text{on} \quad y = 1$$

$$\frac{\partial\theta}{\partial y} = 0 \quad at \quad y = 0 \tag{2.10}$$

The value of ψ on the boundary assumes the constant volumetric flow in consistent with the hypothesis(2.9) .Also the wall temperature varies in the axial direction in accordance with the prescribed arbitrary function t .

3.Analysis of the flow:

The perturbation analysis is carried out by assuming that the aspect ratio δ to be small.

We adopt the perturbation scheme and write

$$\psi(x, y) = \psi_0(x, y) + \delta\psi_1(x, y) + \delta^2\psi_2(x, y) + \ldots\ldots\ldots\ldots\ldots$$

$$\theta(x, y) = \theta_0(x, y) + \delta\,\theta_1(x, y) + \delta^2\,\theta_2(x, y) + \ldots\ldots\ldots\ldots\ldots\ldots \tag{3.1}$$

On substituting (3.1) in (2.13) - (2.15) and separating the like powers of δ the equations and respective conditions to the zeroth order are

$$\psi_{0,\,yyyyy} - M_1^2\psi_{0,\,yy} = -G(\theta_{0,y} + NC_{0,y}) \tag{3.2}$$

$$\theta_{o,yy} + \alpha + \frac{PE_c R^2}{G}(\psi_{o,yy})^2 + \frac{PE_c(D^{-1} + M^2)}{G}(\psi_{o,y}^2) = 0 \tag{3.3}$$

With $\psi_0(+1) - \psi(-1) = 1$

$$\psi_{0,\,y} = 0\ ,\ \psi_{0\,,\,x} = 0 \qquad \text{at } y = \pm 1 \tag{3.4}$$

$$\theta_o = 1 \qquad on \quad y = -1$$

$$\theta_o = Sin(x + \gamma t) \quad on \quad y = 1 \tag{3.5}$$

and to the first order are

IJO - INTERNATIONAL JOURNAL OF MATHEMATICS
(ISSN: 2992-4421)
https://ijojournals.com/
Volume 07 Issue 04 || April, 2024 ||
Prakasha.P[1]*

$$\psi_{1,yyyyy} - M_1^2\psi_{1,yy} = -G\theta_y + (\psi_{0,y}\psi_{0,xyy} - \psi_{0,x}\psi_{0,yyy}) \quad (3.6)$$

$$\theta_{1,yy} = (\psi_{0,x}\theta_{o,y} - \psi_{0,y}\theta_{ox}) + \frac{2PE_cR^2}{G}(\psi_{0,yy}.\psi_{1,yy}) + \frac{2PE_cD^{-1}}{G}(\psi_{0,y}.\psi_{1,y}) \quad (3.7)$$

with

$$\psi_{1(+1)} - \psi_{1(-1)} = 0$$
$$\psi_{1,y} = 0,\ \psi_{1,x} = 0 \text{ at } y = \pm 1 \quad (3.8)$$
$$\theta_1(\pm 1) = 0 \text{ at } y = \pm 1 \quad (3.9)$$

Assuming Ec<<1 to be small we take the asymptotic expansions as

$$\begin{aligned} \psi_0(x,y) &= \psi_{00}(x,y) + Ec\psi_{01}(x,y) + \ldots\ldots\ldots\ldots \\ \psi_1(x,y) &= \psi_{10}(x,y) + Ec\psi_{11}(x,y) + \ldots\ldots\ldots\ldots \\ \theta_0(x,y) &= \theta_{00}(x,y) + \theta_{01}(x,y) + \ldots\ldots\ldots\ldots \\ \theta_1(x,y) &= \theta_{10}(x,y) + \theta_{11}(x,y) + \ldots\ldots\ldots\ldots \end{aligned} \quad (3.10)$$

Substituting the expansions(3.10) in equations (3.2)-(3.9) and separating the like powers- of Ec we get the following

$$\theta_{00,yy} = -\alpha \quad , \quad \theta_{00}(-1) = 1, \theta_{00}(+1) = SinD_1 \quad (3.11)$$

$$\begin{aligned} &\psi_{00,yyyy} - M_1^2\psi_{00,yy} = -G\theta_{00,y} \quad ,\psi_{00}(+1) - \psi_{00}(-1) = 1 \\ &\psi_{00,y} = 0, \psi_{00,x} = 0 \ \ at \ \ y = \pm 1 \end{aligned} \quad (3.12)$$

$$\theta_{01,yy} = -\frac{PR}{G}\psi^2_{00,yy} - \frac{PD^{-1}}{G}\psi^2_{00,y} \quad , \quad \theta_{01}(\pm 1) = 0 \quad (3.13)$$

$$\begin{aligned} &\psi_{01,yyyy} - M_1^2\psi_{01,yy} = -G\theta_{01,y} \quad ,\psi_{01}(+1) - \psi_{01}(-1) = 0, \\ &\psi_{01,y} = 0, \psi_{01,x} = 0 \ \ at \ \ y = \pm 1 \end{aligned} \quad (3.14)$$

$$\theta_{10,yy} = (\psi_{00,y}\theta_{00,x} - \psi_{00,x}\theta_{00,y}) \qquad \theta_{10}(\pm 1) = 0 \quad (3.15)$$

$$\begin{aligned} &\psi_{10,yyyy} - M_1^2\psi_{10,yy} = -G\theta_{10,y} + (\psi_{00,y}\psi_{00,xyy} - \psi_{00,x}\psi_{00,yyy}), \\ &\qquad \psi_{10}(+1) - \psi_{10}(-1) = 0, \psi_{10,y} = 0, \psi_{10,x} = 0 \ \ at \ \ y = \pm 1 \end{aligned} \quad (3.16)$$

$$\begin{aligned} \theta_{11,yy} &= (\psi_{00,y}\theta_{01,x} - \psi_{01,x}\theta_{00,y} + \theta_{00,x}\psi_{01,y} - \theta_{01,y}\psi_{0,x}) - \frac{2PR^2}{G}\psi_{00,yy}\psi_{10,yy} \\ &\qquad - \frac{2PD^{-1}}{G}\psi_{00,y}\psi_{10,y} \ , \theta_1(\pm 1) = 0 \end{aligned} \quad (3.17)$$

$$\begin{aligned} &\psi_{11,yyyy} - M_1^2\psi_{1,yy} = -G\theta_{1,y} + (\psi_{00,y}\psi_{11,xyy} - \psi_{00,x}\psi_{01,yyy} \\ &\qquad + \psi_{01,y}\psi_{00,xyy} - \psi_{01.x}\psi_{00,yyy}), \\ &\psi_{11}(+1) - \psi_{11}(-1) = 0, \psi_{11,y} = 0, \psi_{11,x} = 0 \ \ at \ \ y = \pm 1 \end{aligned} \quad (3.18)$$

4. Shear stress and Nusselt number

The shear stress on the channel walls is given by

$$\tau = \mu\left(\frac{\partial u}{\partial y} + \frac{\partial v}{\partial x}\right)_{y=\pm L}$$

IJO - INTERNATIONAL JOURNAL OF MATHEMATICS
(ISSN: 2992-4421)
Prakasha.P[1]*
https://ijojournals.com/ Volume 07 Issue 04 || April, 2024 ||

which in the non- dimensional form reduces to

$$\tau = \left(\frac{\tau}{\frac{\mu U}{a}} \right) = (\psi_{yy} - \delta^2 \psi_{xx})$$

$$= [\psi_{00,yy} + Ec\psi_{01,yy} + \delta(\psi_{10,yy} + Ec\psi_{11,yy} + O(\delta^2)]_{y=\pm 1}$$

and the corresponding expressions are

$$(\tau)_{y=+1} = d_3 + Ecd_4 + \delta d_5 + O(\delta^2)$$

$$(\tau)_{y=-1} = d_6 + Ecd_7 + \delta d_8 + O(\delta^2)$$

The local rate of heat transfer coefficient(Nusselt number Nu) on the walls has been calculated using the formula

$$Nu = \frac{1}{\theta_m - \theta_w} \left(\frac{\partial \theta}{\partial y} \right)_{y=\pm 1} \qquad \text{Where} \quad \theta_m = 0.5 \int_{-1}^{1} \theta \, dy$$

and the corresponding expressions are

$$(Nu)_{y=+1} = \frac{(m_1 + Ecm_2 + \delta m_3)}{(m_4 + Ec\ m_5 + \delta m_6)}, \quad (Nu)_{y=-1} = \frac{(m_7 + Ec\ m_8 + \delta m_9)}{(m_{10} + Ecm_5 + \delta m_6)}$$

5. Discussion of the Numerical results:

The aim of this analysis is to discuss the effect of the dissipation on the convective flow and heat transfer of a viscous fluid through a porous medium confined in a vertical channel whose walls a travelling thermal wave is imposed. Assuming the Eckert number Ec <<1 the coupled momentum and energy equations have been solved. The velocity and temperature distributions are analysed for different sets of the governing parameters.

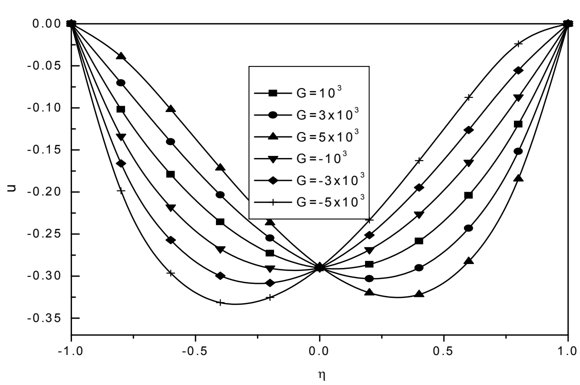

Fig (1) Variation of u with G
R=35, M=2, β=0.5, γ=2, x=π/4, N_1=4, t=π/4

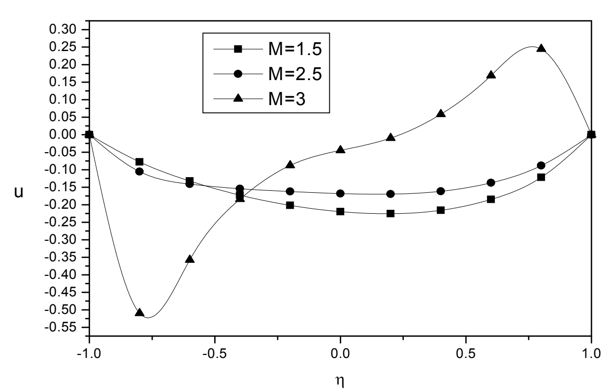

Fig (2) Variation of u with M
G=2x10^3, R=35, β=0.5, γ=2, x=π/4, N_1=4, t=π/4

IJO - INTERNATIONAL JOURNAL OF MATHEMATICS
(ISSN: 2992-4421)
https://ijojournals.com/ Volume 07 Issue 04 || April, 2024 ||
Prakasha.P[1]*

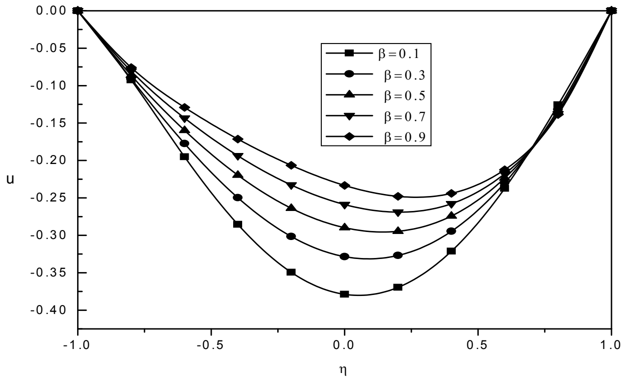

Fig (3) Variation of u with β
G=2x10^3, R=35, M=2,γ=2, x=π/4, N_1=4, t=π/4

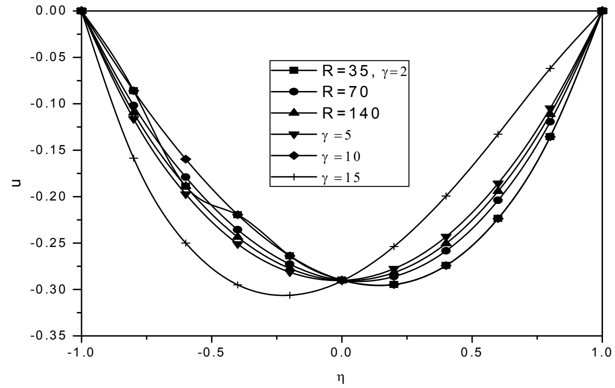

Fig (4) Variation of u with R & γ
G=2x10^3, M=2, β=0.5, x=π/4, N_1=4, t=π/4

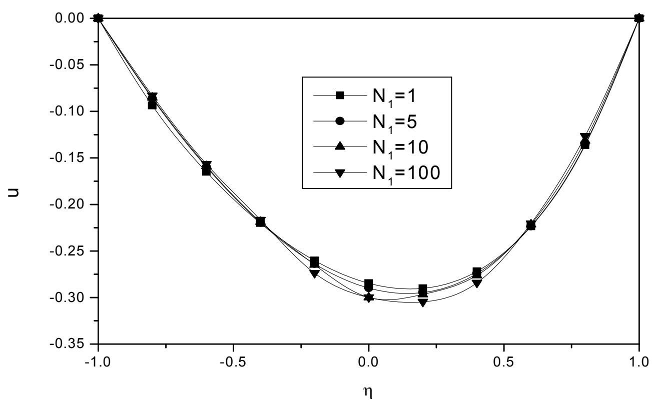

Fig (5) Variation of u with N_1
G=2x10^3, R=35, M=2, β=0.5, γ=2, x=π/4, t=π/4

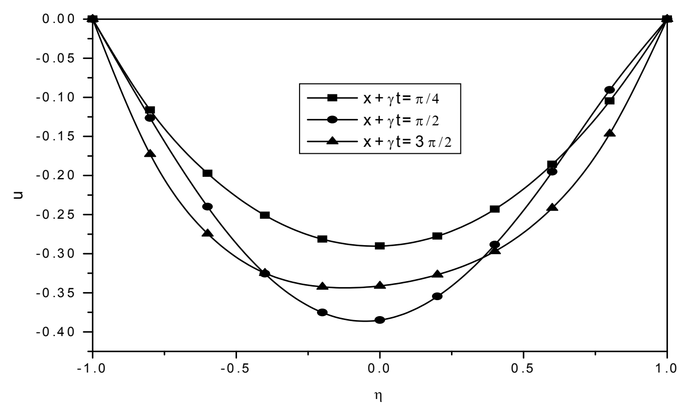

Fig (6) Variation of u with x+ γ t
G=2x10^3, R=35, M=2, β=0.5, γ=5, N_1=4, t=π/4

Fig. (1) exhibits the variation of u with Grashof number G. It is found that the axial velocity u is completely negative for all values of G with maximum occurring at the mid plane y=0 which drifts towards the upper plate for higher G(>0) and it drifts towards the lower boundary for |G|(<0). The magnitude of 'u' reduces in the lower half and enhances in the upper half with an increase in G, while a reversed effect is observed with increase in |G|(<0). The variation of 'u' with M shows that for lower values of the Hartman number M we find reversed flow in the vicinity of both the boundaries and for higher M~O(1.5) the reversed flow in the vicinity of upper boundary disappears and reversal flow continues in the vicinity of lower boundary and for still higher values of M≤3 the reversal flow disappears in the entire flow region. For M=5.0 the reversal flow reappears in the vicinity of upper boundary. This shows that under the influence of strong magnetic field the free convection effect do not dominate over others. An increase in M~O(1.5) enhances 'u' in entire fluid region and for further increase in M(≥2.5) we find depreciation in |u| in the flow region. From fig. (3) we find that greater the dilation lesser the

IJO - INTERNATIONAL JOURNAL OF MATHEMATICS
(ISSN: 2992-4421)
https://ijojournals.com/
Volume 07 Issue 04 || April, 2024 ||

Prakasha.P[1]*

magnitude of u. An increase in the Reynolds number R leads to an enhancement |u| in the lower half and depreciation in the upper half. Also an increase in the thermal wave velocity $\gamma(\leq 10)$ depreciates |u| in the lower half and enhances in the upper half and for higher $\gamma(\geq 15)$ a reversed effect is observed in the flow region (fig. (4)). The variation of 'u' with radiation parameter N_1 shows a reversal flow in the mid region for smaller values of N_1 and this reversal flow disappears for higher values of N_1. |u| reduces in the lower half and enhances in the upper half with $N_1(\leq 1.0)$ and for higher $N_1(\geq 5)$ we notice a depreciation in |u| in the region abutting the boundaries and an enhancement in the mid region (fig.(5)). The variation of u with the phase x+γt of the boundary temperature curve, shows that |u| enhances with $x+\gamma t \leq \frac{7\pi}{4}$ and for higher values of x+γt we notice an enhancement in the vicinity of the boundary and depreciation in the mid region. (Fig.6)

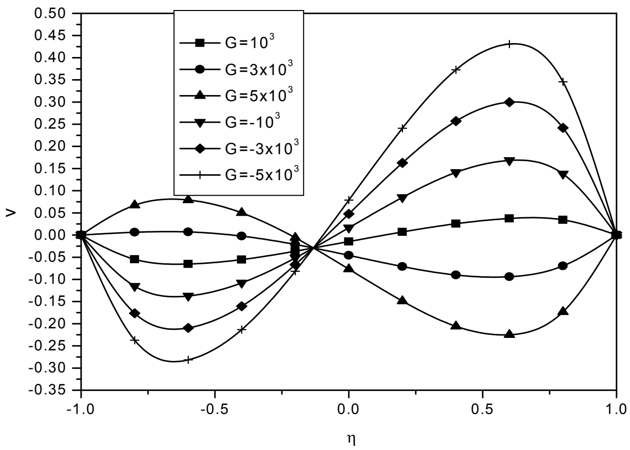

Fig (7) Variation of v with G
R=35, M=2, β=0.5, γ=2, x=π/4, N_1=4, t=π/4

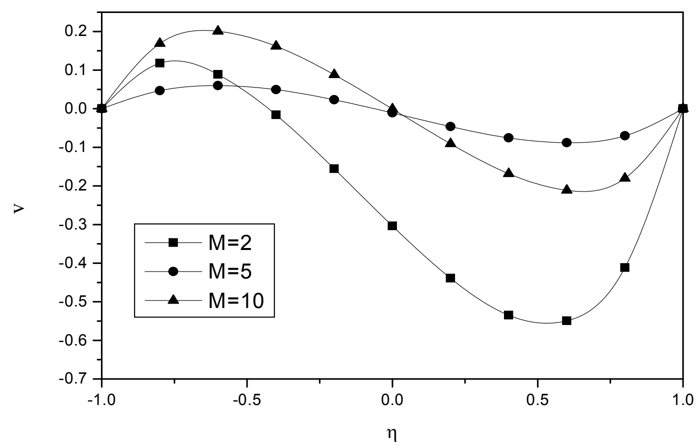

Fig (8) Variation of v with M
G=2x10^3, R=35, β=0.5, γ=2, x=π/4, N_1=4, t=π/4

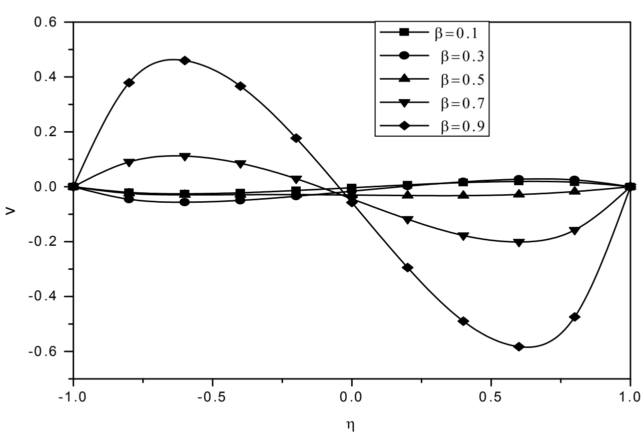

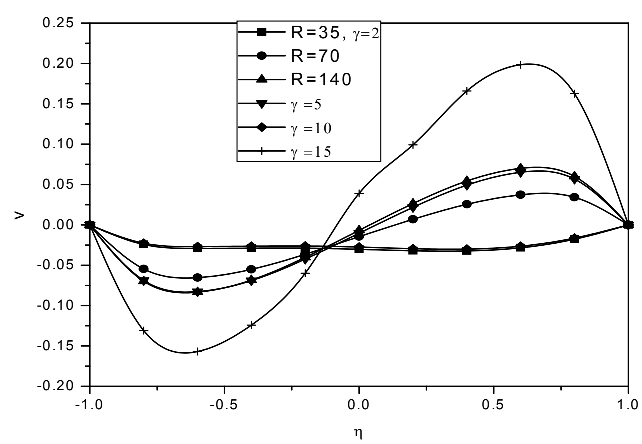

IJO - INTERNATIONAL JOURNAL OF MATHEMATICS
(ISSN: 2992-4421)
https://ijojournals.com/
Volume 07 Issue 04 || April, 2024 ||
Prakasha.P[1]*

Fig (9) Variation of v with β
G=2x10^3, R=35, M=2, γ=2, x=π/4, N_1=4, t=π/4

Fig (10) Variation of v with R & γ
G=2x10^3, M=2, β=0.5, x=π/4, N_1=4, t=π/4

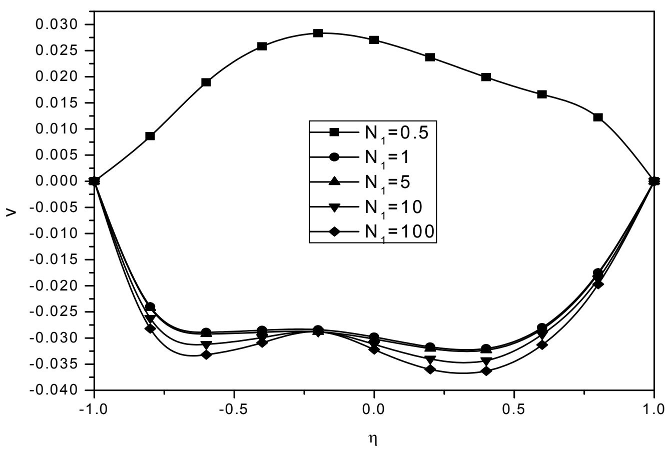

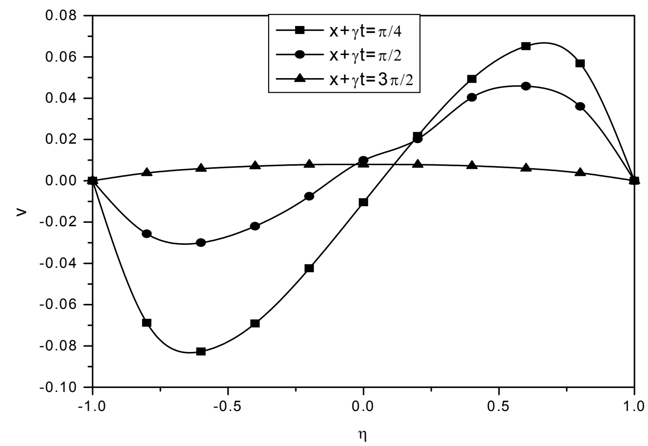

Fig (11) Variation of v with N_1
G=2x10^3, R=35, M=2, β=0.5, γ=2, x=π/4, t=π/4

Fig (12) Variation of v with x+ γ t
G=2x10^3, R=35, M=2, β=0.5, γ=5, N_1=4, t=π/4

The secondary velocity 'v' which arises due to the non-uniformity in the boundary has been depicted in figs. (7) - (12) for different G,R,M,γ,β,N_1 and x+γt. We notice that for smaller G(≤10^3) the secondary velocity in the left half and in the upper region it is directed towards the boundary. For higher G(≥3x10^3) the fluid in the left half is directed towards the boundary and the fluid in the upper half is directed towards the mid region, while for |G| (<0) the fluid in the left half is directed towards the mid region and the fluid in the upper half is directed towards boundary, for all |G|.

The variation of 'v' with M shows that for smaller values of M~O(0.5) the fluid in entire flow region is directed towards the mid region, while for higher M(≥1.5) the fluid in the flow region is towards the boundary except in the vicinity of the left boundary is directed towards the mid region. The region where the transition takes place enhances its size with increase in M. An increase in M~O(3.5) we find a retardation in |v| and for further increase in M the velocity v in the left region experiences a depreciation and that in the right region experiences an enhancement and for still higher M(≥5) we find an enhancement in |v| in the entire flow region (fig. (8)). From fig. (9), it is found that greater the dilation β~O(3.5) larger the |v| and for higher β~O(0.5) we notice a depreciation in |v| in the left half and enhancement in |v| in the right half and for still higher β, larger |v| in entire flow region. An increase in R enhances |v|. Also an increase in the thermal wave velocity γ enhances |v| in the upper half and reduces it in the lower half, and for further increase in γ we find an enhancement in |v| (fig. (10)). The variation 'v' with N_1 shows that for small values of N_1 the secondary velocity is directed towards the boundary and for higher values of N_1 we find that v is towards the mid region for all N_1. |v| enhances with increase in N_1. (fig. (11)). The variation 'v' with phase x+γt of the boundary curve shows that for increasing $x+\gamma t \le \frac{7\pi}{4}$ the velocity in the left half reduces and that in the right region enhances with x+γt and for higher values of $x+\gamma t \ge \frac{11\pi}{4}$ we find an increase in |v|. (Fig.12) .

IJO - INTERNATIONAL JOURNAL OF MATHEMATICS
(ISSN: 2992-4421)
https://ijojournals.com/
Volume 07 Issue 04 || April, 2024 ||

Prakasha.P[1]*

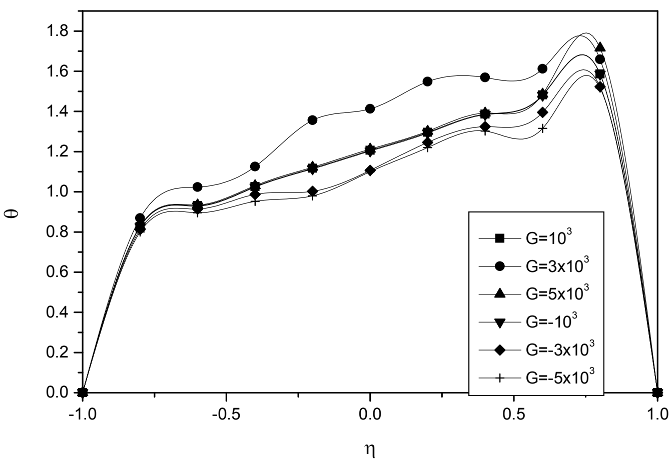

Fig (13) Variation of θ with G
$R=35$, $M=2$, $\beta=0.5$, $\gamma=2$, $x=\pi/4$, $N_1=4$, $t=\pi/4$

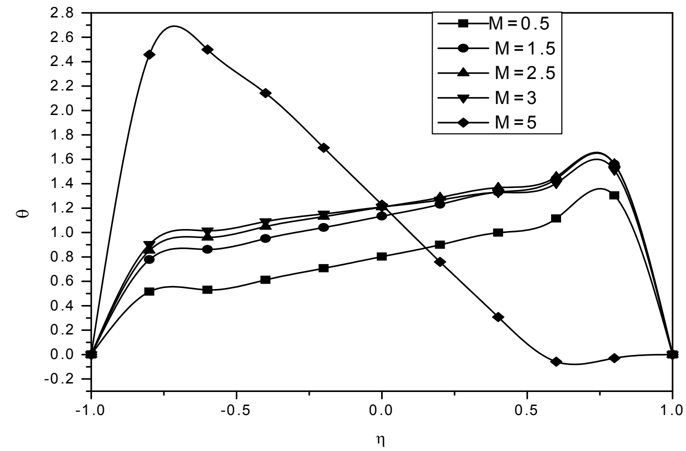

Fig (14) Variation of θ with M
$G=2x10^3$, $R=35$, $\beta=0.5$, $\gamma=2$, $x=\pi/4$, $N_1=4$, $t=\pi//4$

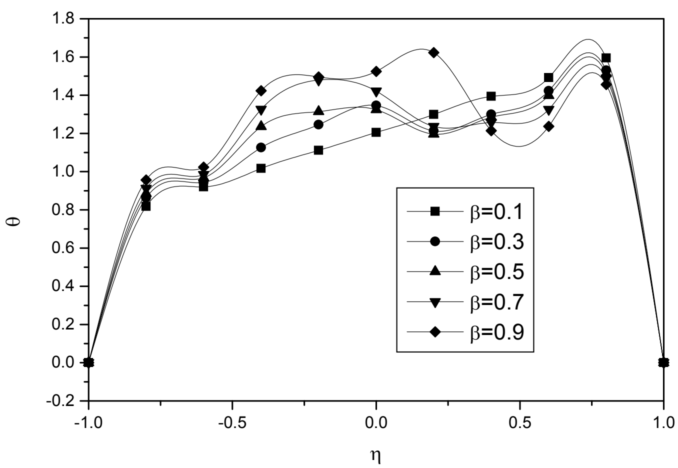

Fig (15) Variation of θ with β
$G=2x10^3$, $R=35$, $M=2$, $\gamma=2$, $x=\pi/4$, $N_1=4$, $t=\pi/4$

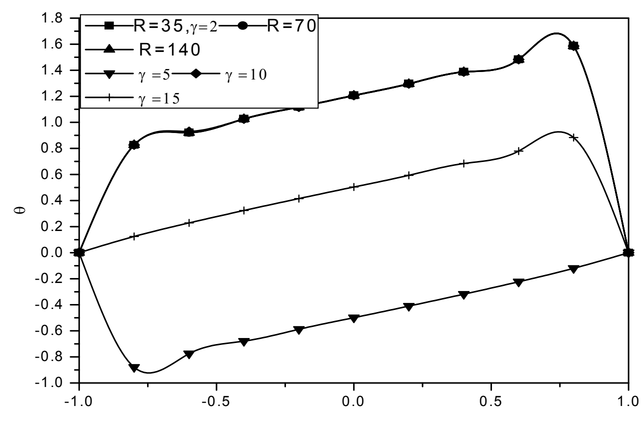

Fig (16) Variation of θ with R & γ
$G=2x10^3$, $M=2$, $\beta=0.5$, $x=\pi/4$, $N_1=4$, $t=\pi/4$

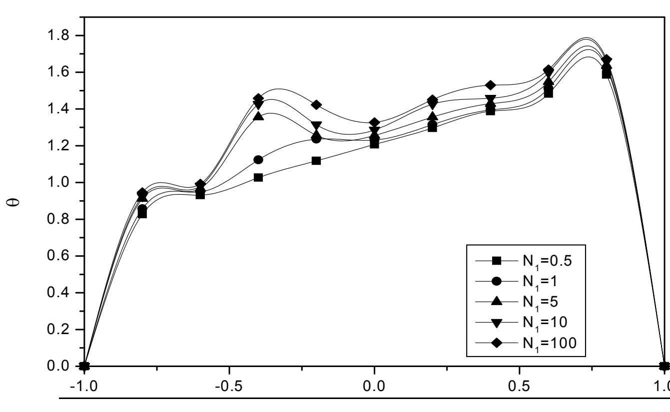

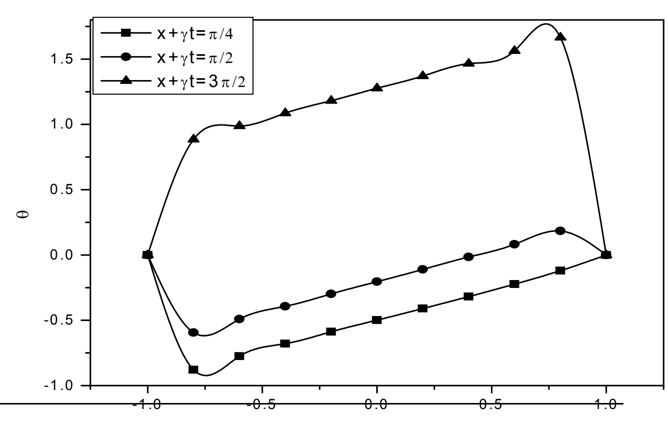

IJO - INTERNATIONAL JOURNAL OF MATHEMATICS
(ISSN: 2992-4421)
https://ijojournals.com/ Volume 07 Issue 04 || April, 2024 ||
Prakasha.P[1]*

Fig (17) Variation of θ with N_1
$G=2x10^3$, R=35, M=2, β=0.5, γ=2, x=π/4, t=π/4

Fig (18) Variation of θ with x+ γ t
$G=2x10^3$, R=35, M=2, β=0.5, γ=5, N_1=4, t=π/4

The temperature distribution (θ) for different values of G,R,M,β,N_1 and x+γt is shown in figs. (13) - (18). The perturbation temperature in general is positive and hence contributes to the enhancement of actual temperature in the fluid region. Fig (13) depicts behavior of θ for different |G|(><0). We notice that in a dilated channel the temperature increases/decreases with |G| according as with G(>0) or G(<0). An increase in M~O(2.5) we find an enhancement in θ. For higher M(≥3.0) the temperature in the left half enhances and that in the right half depreciates with increase in M. Also higher the dilation larger the temperature in the left region and smaller the temperature in the upper region (fig.(15)). An increase in R decreases θ. The variation of 'θ' with γ shows that for γ≤5 the temperature is negative and for higher γ≤10, θ is positive. Also an increase in γ≥10 leads to an enhancement in 'θ' and for further higher values of γ we notice a depreciation in θ. The effect of radiation on 'θ' is shown in fig. (17). An enhancement in the radiation parameter N_1 results in an increase in the temperature in entire flow region. The variation of θ with phase x+γt of the boundary temperature curve shows that for $x+\gamma t \geq \frac{\pi}{2}$ the temperature is negative and for higher values of x+γt, θ is positive. For an increase $x+\gamma t \leq \frac{\pi}{2}$ we find depreciation in θ and for higher $x+\gamma t \geq \frac{3\pi}{2}$, θ enhances in entire flow field(Fig.18).

Table.1 Shear stress(τ) at y = 1 , P=0.71

G	I	II	III	IV	V	VI	VII	VIII
10^3	-27.32	-54.318	-86.19	-38.688	-49.176	-27.303	-49.182	-59.912
$3x10^3$	53.5904	-83.733	-106.441	-75.856	-88.87	53.501	-108.481	-127.611
$5x10^3$	84.3505	-122.711	-176.981	-100.541	-123.291	93.685	-236.881	-168.051
-10^3	-54.375	-62.796	-89.806	-43.128	-59.124	-54.393	-71.123	-66.969
$-3x10^3$	-76.578	-97.488	-102.951	-83.242	-108.591	-76.647	-177.041	-87.759
$-5x10^3$	-144.941	-167.721	-251.611	-159.061	-168.491	-128.711	-281.771	-196.321

Table.2 Shear stress(τ) at y = -1 P=0.71

G	I	II	III	IV	V	VI	VII	VIII
10^3	0.0857	0.5203	0.8311	0.6351	-1.1167	0.0494	-1.2606	0.5973
$3x10^3$	3.6351	-2.3797	-6.0387	-2.9492	-6.9704	3.2407	-9.6896	-3.1505
$5x10^3$	33.614	4.6238	-10.804	-3.5669	4.9161	32.0035	-7.2413	1.1336
-10^3	3.1566	3.6622	3.8092	2.3599	1.8977	3.1929	2.0418	3.7117
$-3x10^3$	-6.9607	-2.6153	-3.0992	-2.6016	-18.506	-6.5656	-15.785	-2.4721
$-5x10^3$	-50.075	-27.973	-25.889	-19.076	-82.909	-48.462	-70.746	-26.619

IJO - INTERNATIONAL JOURNAL OF MATHEMATICS
(ISSN: 2992-4421)
https://ijojournals.com/
Volume 07 Issue 04 || April, 2024 ||
Prakasha.P[1]*

	I	II	III	IV	V	VI	VII	VIII
D^{-1}	10^3	$2x10^3$	$3x10^3$	10^3	10^3	10^3	10^3	10^3
γ	5	5	5	15	5	5	5	5
α	2	2	2	2	5	-2	-5	2
M	2	2	2	2	2	2	2	4

Table.3 Average Nusselt Number(Nu) at y = 1 P=0.71

G	I	II	III	IV	V	VI	VII	VIII
10^3	-0.9304	-1.2347	-1.6751	-0.7476	-1.0113	-5.6211	-1.6412	-1.3149
$3x10^3$	-0.6146	-0.9777	-1.3334	-0.5734	-0.6634	-3.9777	-3.0481	-1.0412
$5x10^3$	0.2125	-0.7692	-1.2206	-0.2668	0.5107	-3.5075	-2.7442	-0.8637
-10^3	-0.9312	-1.2373	-1.6772	-0.7435	-1.0099	-3.1893	-1.6391	-1.3176
$-3x10^3$	-0.6105	-0.9761	-1.3324	-0.5467	-0.6578	-5.5872	-2.0022	-1.0398
$-5x10^3$	0.2239	-0.7658	-1.2185	-0.1927	0.5286	-3.9744	-2.3682	-0.8607

Table..4 Average Nusselt Number (Nu) at y = -1 P=0.71

G	I	II	III	IV	V	VI	VII	VIII
10^3	4.1254	3.7439	3.6133	1.8222	2.2733	1.1622	1.4049	3.6995
$3x10^3$	5.7579	3.9748	3.9277	1.6329	1.7193	1.4569	1.6775	3.9398
$5x10^3$	2.6433	3.9312	3.8872	1.2358	-9.867	1.8127	2.0487	3.8663
-10^3	4.1209	3.7371	3.6112	1.7882	2.2721	1.1636	1.4041	3.6961
$-3x10^3$	5.7866	3.9729	3.9265	1.5031	1.7107	1.4549	1.6752	3.9381
$-5x10^3$	2.6557	3.9271	3.8852	0.8944	-10.557	1.8103	2.0461	3.8624

	I	II	III	IV	V	VI	VII	VIII
D^{-1}	10^3	$2x10^3$	$3x10^3$	10^3	10^3	10^3	10^3	10^3
γ	5	5	5	15	5	5	5	5
α	2	2	2	2	5	-2	-5	2
M	2	2	2	2	2	2	2	4

The shear stress (τ) and the average Nusselt number (Nu) on the boundaries ($y= \pm1$) have been evaluated for different parameters and are given in tables (1)-(4). The shear stress is positive at y = -1 and negative at y = 1. It is found that τ is observed to increase with an increase in G fixing the other parameters. Higher the permeability of the medium larger the shear stress at both the boundaries. With reference to α we find that τ increases for an increase in α for all G (tables 1 & 2).

The average Nusselt number measures the local rate of heat transfer across the boundary. We find from (tables.3 & 4) that the average Nusselt number is positive at y = 1 and negative at y = -1 for all variations. The magnitude of Nu at $y= \pm 1$ increases with an increase in G > 0 and decreases with G<0 fixing the other paramerters. In axial heating case Nu decreases with R and enhances with D^{-1} while a reversed effect is observed in the case of axial cooling. The rate of heat transfer (Nu) declines with an increase in the amplitude α of the boundary temperature (tables.3&4).

IJO - INTERNATIONAL JOURNAL OF MATHEMATICS
(ISSN: 2992-4421)
https://ijojournals.com/ Volume 07 Issue 04 || April, 2024 ||

Prakasha.P[1]*

6.References

[1] Barletta,Antonio , Laminar mixed convection with viscous dissipation in a vertical channel., *Int.J.Heat and Mass transfer*,41,No.22,pp.3501-3513,(1998).
[2] Barletta,Antonio , Combined forced and free convection with viscous dissipation in a vertical circular duct., *Int.J.Heat and Mass Transfer*,42,No.12,pp.2243-2253,(1999).
[3] Bulent Yesilata , Effect of viscous dissipation on polymeric flows between two rotating Coaxial parallel discs., *Int.Comm. Heat and Mass Transfer*, 29, No.29, No.5, pp.589- 600,(2002).
[4] El-Hakein, M.A., Viscous dissipation effects on MHD free convection flow over a non-isothermal surface in a micropolar fluid. *Int.Comm.Heat and Mass Transfer* ,27, No,4 pp.581-590,(2000).
[5] Israel-Cookey ,C. , Influence of viscous dissipation and radiation on unsteady MHD free convection flow past an infinite heated vertical plate in a porous medium with time-dependent suction.,*Int.J.Heat and Mass Transfer,*46,No.13,pp.2305-2311,(2003).
[6] Rossie di Schio,Baletta,A,Hahne,E and Spindler,K , Analysis of the effect of viscous dissipation for laminar flow in Stadium –shaped ducts, *Int.Comm.Heat Mass Transfer,*28, No.4, pp.449-459,(2001).
[7] Chen, C. H. Laminar mixed convection adjacent to vertical, continuously stretching sheets. Heat and Mass Transfer, 33(5-6), 471–476 (1998)
[8] Elbashbeshy, E. M. A. and Bazid, M. A. A. Heat transfer over an unsteady stretching surface.Heat and Mass Transfer, 41(1), 1–4 (2004)
[9] Sharidan, S., Mahmood, T., and Pop, I. Similarity solutions for the unsteady boundary layer flow and heat transfer due to a stretching sheet. International Journal of Applied Mechanics and Engineering, 11(3), 647–654 (2006)
[10] Tsai, R., Huang, K. H., and Huang, J. S. Flow and heat transfer over an unsteady stretching surface with a non-uniform heat source. International Communications in Heat and Mass Transfer,35(10), 1340–1343 (2008)
[11] Ishak, A., Nazar, R., and Pop, I. Hydromagnetic flow and heat transfer adjacent to a stretching vertical sheet. Heat and Mass Transfer, 44(8), 921–927 (2008)
[12] Aziz, A. A similarity solution for laminar thermal boundary layer over a flat plate with a convective surface boundary condition. Communications in Nonlinear Science and Numerical Simulation,14(4), 1064–1068 (2009)
[13] Chen, C. H. Combined heat and mass transfer in MHD free convection from a vertical surface with Ohmic heating and viscous dissipation. International Journal of Engineering Science, 42(7),699–713 (2004)
[14] Pal, D. and Hiremath, P. S. Computational modelling of heat transfer over an unsteady stretching surface embedded in a porous medium. Meccanica, 45(3), 415–424 (2010)
[15] Veena, P. H., Subhas-Abel, M., Rajagopal, K., and Pravin, V. K. Heat transfer in a visco-elastic,fluid past a stretching sheet with viscous dissipation and internal heat generation. Zeitschrift f¨ur,Angewandte Mathematik und Physik (ZAMP), 57(3), 447–463 (2006)
[16] Palani, G. and Ganesan, P. Heat transfer effects on dusty gas flow past a semi-infinite inclined,plate. Forsch Ingenieurwes, 71, 223–230 (2007)